

# MEASUREMENT OF BENDING IN SPECIMENS OF CERAMIC-MATRIX COMPOSITES UNIAXIALLY LOADED IN TENSION-COMPRESSION

P. Reynaud<sup>1</sup>, C. Tallaron<sup>2</sup>, A. Cosculluela<sup>2</sup>  
C. Cambas<sup>3</sup>, P. Gomez<sup>3</sup>, J.L. Delamaide<sup>3</sup>, M. Bourgeon<sup>4</sup>

<sup>1</sup>*Groupe d'Etudes de Métallurgie Physique et de Physique des Matériaux, U.M.R. C.N.R.S.  
5510, I.N.S.A. de Lyon, F69621 Villeurbanne Cedex, France*

<sup>2</sup>*Commissariat à l'Energie Atomique, CEA Le Ripault, BP n°16, F37260 Monts, France*

<sup>3</sup>*Centre d'Essais Aéronautique de Toulouse, F31130 Balma, France*

<sup>4</sup>*Société Européenne de propulsion, BP 37, F33165 S<sup>t</sup> Médard en Jalles, France*

**SUMMARY:** When a uniaxial test under tension or compression is performed, the uniformity of the longitudinal stress field in specimens is of major importance. Every imperfection of the testing system as misalignment of grips, or as bad orientation of gripping planes, induces a perturbation of the stress field in the working part of the specimen due to a parasite bending.

To be valid, a tensile testing system shall apply on specimens a percent of bending strain (PBS) lower than a critical value. The aim of this work is to study the effects of imperfections of the gripping system on the level of the PBS, and to determine the easiest experimental procedure to measure the PBS on a specimen (number and localisation of strain gauges). This study has been done with finite elements codes in order to simulate the defects applied on the specimens by the gripping system.

**KEYWORDS:** ceramic matrix composite, measurement, tensile, testing.

## INTRODUCTION

To measure a mechanical property of a material (for example the Young's modulus), a specific stress field should be applied on the material, and this field should be as close as possible of the theoretical field we want to apply. Hence, in order to have the best accuracy, a great care have to be taken on the setting of the loading train. For example, on a uniaxial tensile test the stress field applied on the material have to be a uniform field of longitudinal stress. In that case, discrepancy between experimental and theoretical stress field is induced by a misalignment of grips, that apply a parasite bending. Hence, for a good measurement, this bending have to be as low as possible, and for a given acceptable error of measurement, have to be lower than a critical value we want to determine.

## SOURCES OF MISALIGNMENT

Bending caused by a misalignment of grips in the test piece-grip-loading train-frame assembly is pernicious for the measurement of tensile properties and is one of the principal causes of scatter. This work is concentrated on the sources of error caused by the grip to grip non-coaxiality which can take two forms : the concentricity error and the angularity error (fig. 1).

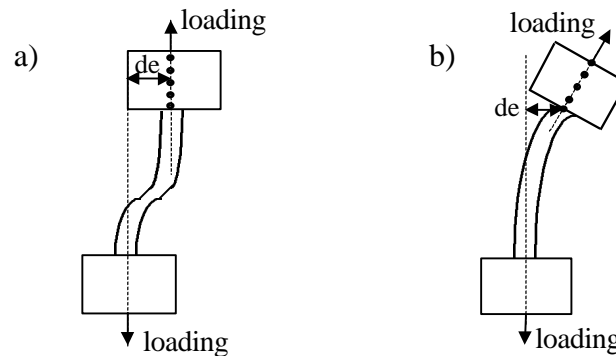


*Fig 1 : Schematic representation of grips misalignment  
a) concentricity error, b) angularity error*

## FINITE ELEMENT ANALYSIS

Based on the schematic representation of fig.1, the aim of this study is to numerically model the effect of the two sources of misalignment described above. With a 3D finite element analysis, bending caused by misalignment can be modelled and some important factors which modify the strain field in the specimen can be highlighted.

The concentricity and angularity errors are independently treated, and different parameters are considered as the stiffness or as the geometry of the specimen used. The percent bending strain (PBS) is determined with the elastic strains calculated in the working part of the specimen at specific location and using the theoretical expressions given in [1] for thin rectangular test-piece (see PBS calculation).

### Specimen geometry

The specimen geometry is a parallelepipedic shape of 195 mm in length, 18 mm in width and 4 mm in thickness. The working part length is of 100 mm and each gripping part is of 47.5 mm length (Fig 2). The stiffness of the specimen is  $144 \text{ N.m}^{-1}$ .

The 3D finite element calculations are performed using two softwares (ANSYS and CASTEM). For both code, the specimen geometry is built using cubic finite elements of 8 nodes. Each element is of 4 mm in length and 2 mm in width. In order to precisely obtain the strains on the specimen wide face (front and back) as electric strain gauges during an experimental test, the strains are calculated on the surface with ANSYS by using a finite element named "solid45" which allow us to directly obtain the strain on the surface. This option is not possible with CASTEM. In that case, our choice is to mesh 10 elements named "Cu8" in the thickness of the specimen. By this way, the strains are taken on the element located on the surface. An example of element locations in a section where the strains are raised is shown fig. 2 (detail of Section T). Three sets of cubic elements are considered for strain evaluation. The specimen having an uniform cross section, the strains are taken at the middle of the working part (Section M, for Middle), at halfway between the middle and the

lower face of the upper grip (section T, for Top) and at halfway between the middle and the upper face of the lower grip (section B, for Bottom).

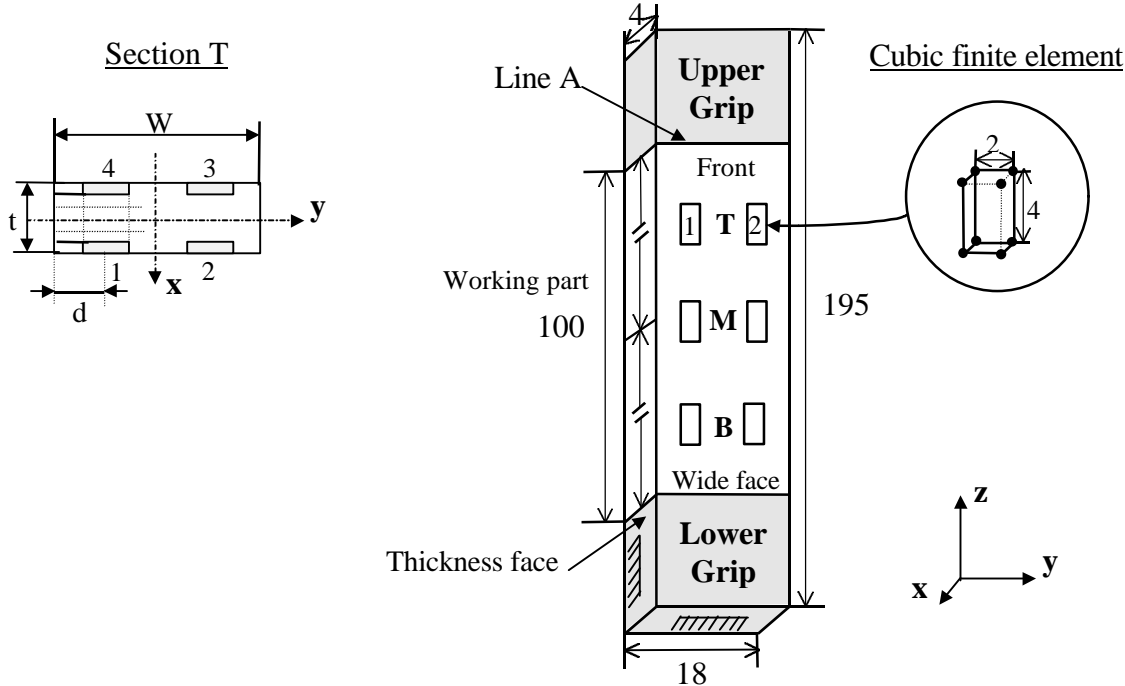


Fig 2 : Specimen geometry modelled by 3D finite element codes.

**Limit conditions and loading cases**

In order to realise a tensile modelling, all displacements of the lower grip are locked. The concentricity error is modelled by imposing to the mesh an eccentricity defect (de), parallel to the x axis, to all nodes of the upper grip. The deformed shape obtained is called the "S-shape" (Fig. 1-a and 3-b). The angularity error is modelled by imposing to the mesh an eccentricity defect (de), parallel to the x axis, to all nodes of line A on the upper grip. The deformed shape obtained is called the "C-shape" (Fig. 1-b and 3-c).

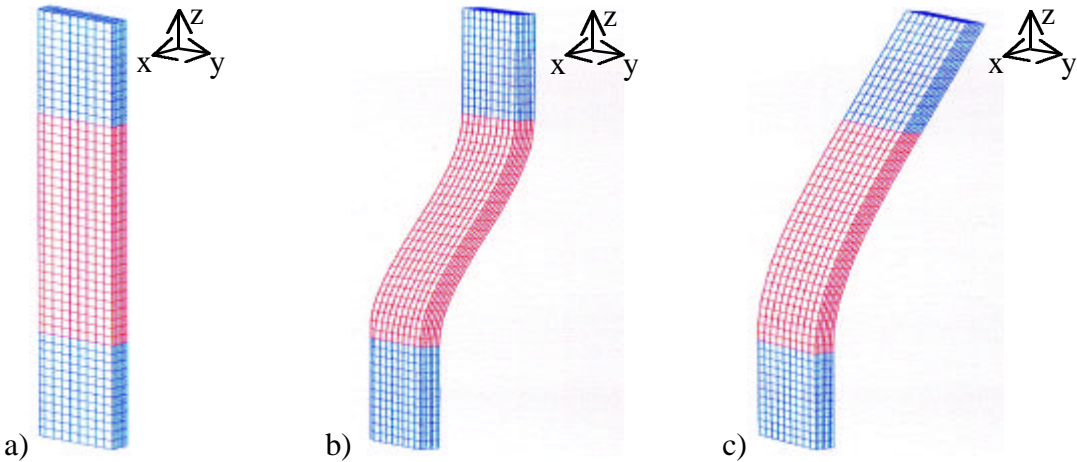


Fig 3 : Deformed meshes calculated with 3D finite element code CASTEM after bending  
 a) Initial mesh ; b) S-shape ; c) C-shape

After application of the non-coaxiality errors, specimen meshes are loaded in tension for different loading cases. From strain evaluations obtained at three cross sections of the specimen (section T, M, and B) and for both loading case, we determined the maximum Percent Bending Strain (PBS) using the theoretical expression briefly given here after.

### Percent bending strain (PBS) analytical calculation

In this part, we give the calculation procedure and the principal theoretical expression used to determine the PBS for a thin rectangular specimen. This description is based on the work of M. Steen [2].

The first step consists in determining the bending strain on the thickness and on the wide faces of the test piece respectively caused by bending about the x axis and the y axis (Eq. 1). The bending strains  $\epsilon_{ix}$  and  $\epsilon_{iy}$  ( $i = T, M, B$ ) are the difference between the longitudinal strain at a given location and the axial strain  $\epsilon_a$ . If the non-coaxiality errors are only applied in the direction of x (that is the case of our study), only  $\epsilon_{ix}$  is not equal to zero.

$$\begin{aligned}\epsilon_{ix} &= \frac{\epsilon_{i1} + \epsilon_{i2}}{2} - \epsilon_a \\ \epsilon_{iy} &= \frac{w}{w - 2d} * \left[ \frac{\epsilon_{i1} + \epsilon_{i4}}{2} - \epsilon_a \right]\end{aligned}\quad (1)$$

The axial strain  $\epsilon_a$  is the average of longitudinal strains retained on the surface for each cross section (see Fig. 2) :

$$\epsilon_a = \frac{1}{4} \sum_{j=1}^4 \epsilon_{ij} \quad \text{for } i = T, M, B \quad (2)$$

The second step is the calculation of the bending moments for each cross section of the test piece. Only the bending moment in the section T and B are useful to calculate the maximum bending moment  $m_S$  and  $m_I$  in the section S and I, respectively defined by the lower face of the upper grip and the upper face of the lower grip (see Fig. 4). The bending moments in the sections T, M and B are determined by Eq. 3.

$$\begin{aligned}m_{ix} &= \epsilon_{iby} * w \\ m_{iy} &= -\epsilon_{ibx} * t\end{aligned}\quad \text{for } i = T, M, B \quad (3)$$

with  $w$  the width and  $t$  the thickness of the specimen.

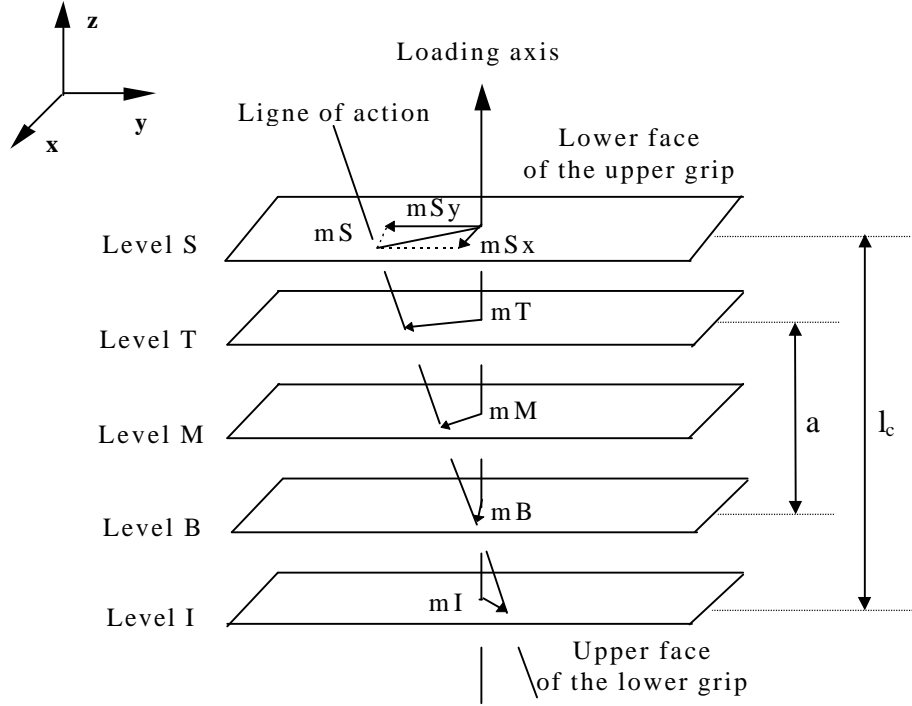


Fig 4 : Representation of bending moments in each cross section

The components of bending moments  $mS$  and  $mI$  are determined by a geometrical projection of  $mT$  and  $mB$  components on the section S and I. The magnitude of the maximum bending moment is calculated as the larger value of the following two expressions :

$$\begin{aligned}
 |mI| &= \sqrt{(1+\lambda)^2 |mB|^2 + \lambda^2 |mT|^2 - 2\lambda(1+\lambda)(mTx * mBx + mTy * mBy)} \\
 |mS| &= \sqrt{(1+\lambda)^2 |mT|^2 + \lambda^2 |mB|^2 - 2\lambda(1+\lambda)(mTx * mBx + mTy * mBy)} \quad (4)
 \end{aligned}$$

with  $\lambda = \frac{l_c - a}{2a}$ , the projection coefficient.

If the magnitude of  $mS$  is higher than the magnitude of  $mI$ , the maximum bending vector B is obtained by Eq. 5.

$$|B| = \frac{mSx}{w} - \frac{mSy}{t} \quad (5)$$

The last step of the calculation is the determination of the PBS which is the bending strain times 100 divided by the axial strain (Eq. 6). As for the bending strain, the percent bending varies from point to point along the parallel length, depending on the projection coefficient  $\lambda$ .

$$PBS = 100 * \frac{|B|}{\epsilon_a} \quad (6)$$

## RESULTS AND DISCUSSION

### Magnitude of PBS

The finite element calculations are performed for the two non-coaxiality errors (S-shape and C-shape), with a magnitude of eccentricity defect ( $d_e = 0.2$  mm) and two cases of loading ( $F = 5$  kN and 10kN). The results obtained from the two softwares (CASTEM and ANSYS) are reported here after.

The two softwares give the same results for the C-shape. A small discrepancy is observed for the S-shape, a larger value of PBS is calculated with CASTEM. This smooth difference probably comes from the limit conditions used. Generally, the PBS decreases with the loading. Effectively, the specimen tends to align with the loading axis when the loading increases. The PBS value is higher for the S-shape than for the C-shape. This results comes from the strain field in each cross section induced by the eccentricity defect. The difference between the strain field in the section T and the strain field in the section B is higher for the S-shape than for the C-shape.

*Table 1 : Synthesis of the maximum PBS calculated for a thin rectangular test piece at different locations along the working part (for  $l_c=100$  mm and  $l_c= 24$  mm)*

$l_c$	F (kN)	PBS (%) -ANSYS-		PBS (%) -CASTEM-	
		S-shape	C-shape	S-shape	C-shape
100	5	66	34	70	34
	10	33	17	35	17
24	5	14	20.8	17	21
	10	7	10.4	8.5	10.5

The magnitude of PBS also depends on the position along the working part. The PBS values obtained for  $l_c$  equal to 24 mm will be used in the next section to show the influence of the PBS on the measurement of the Young's modulus (experimentally measured by an extensometer of 24 mm gauge length).

Two other parameters are studied, in relation to the geometry and the stiffness of the specimen [1]. The results are not detailed in this paper, but general tendencies are given. Increasing the stiffness of the specimen increases the magnitude of PBS for S-shape and C-shape. Decreasing the thickness of the specimen decreases the magnitude of the PBS. Accordingly, an experimental verification of misalignment have to take into account the geometry and the stiffness of the standardised specimen used compare to the geometry and the stiffness of the specimen of the test series.

Because the results of the two codes are relatively close, in the following parts only the calculations of CASTEM are developed.

## Calculation of the critical percent of bending

The aim of this section is to show by calculations the influence of the PBS on the Young's modulus error of measurement on a specimen mechanically tested in tension. Consequently, a critical value of PBS will be given in relation to an acceptable error on the measurement of the Young's modulus.

When an eccentricity defect is applied, for the two non-coaxiality errors (S-shape and C-shape), the meshes are loaded and specific longitudinal nodes displacements are followed. The nodes locations virtually correspond to the position of an extensometer on the thickness face or on the wide face of the specimen (Fig. 5). The calculation on the thickness face simulate an error of the operator when the extensometer is located (+50% or -50% of setting error) as regards to the neutral axis.

The results obtained with CASTEM are reported in table 2. The first important remark is the zero value of the Young's modulus error calculated for the S-shape. This result is explained by the symmetric deformation and then by the symmetric nodes displacements for each nodes line. All nodes lines are deformed like the "neutral axis" (Fig 5).

In the case of the C-shape, the deformation is not symmetric and the Young's modulus error is not symmetric too. This error increases from the basic position (on the neutral axis) to the extreme position (on the front or on the back wide face). These two positions respectively correspond to a minimum and a maximum value of the Young's modulus error. As a consequence, the experimental measurement of the Young's modulus must be performed as close as possible to the neutral axis on the thickness face of the specimen.

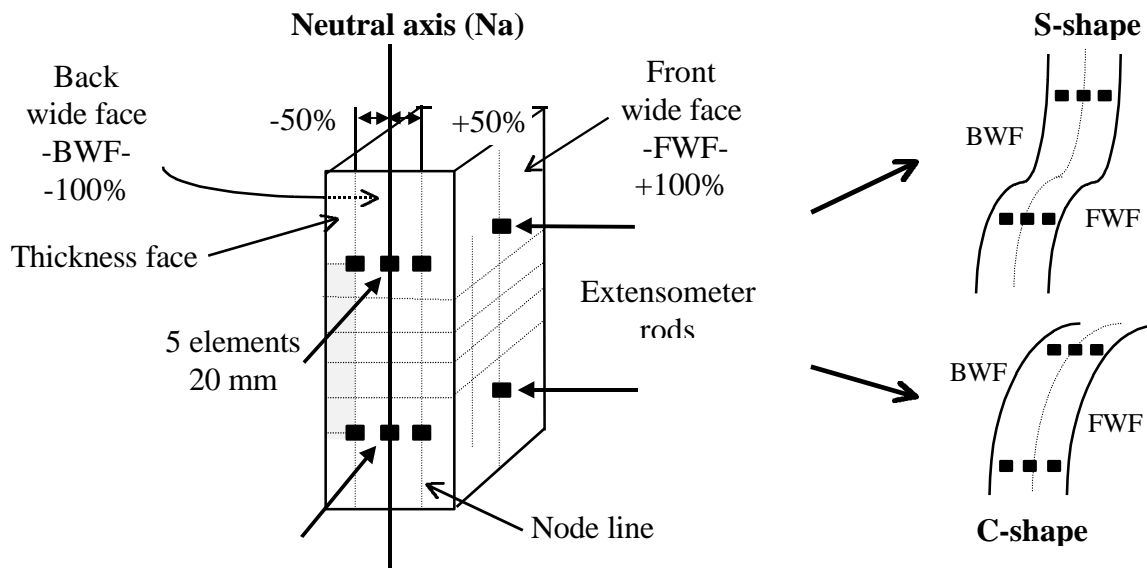


Fig 5 : Nodes location on the working part for the Young's modulus calculation, for S-shape and C-shape.

Table 2 : Synthesis of the Young's modulus and the maximum PBS associated calculated on the extensometer gauge length for different specimen face and for  $de = 0.2\text{mm}$  (\*).

		Location of extensometer rods				
		BWF (-100%)	-50%	Na	+50%	FWF (+100%)
F(kN)	PBS ( $l_c=20\text{mm}$ )	S-shape : Young's modulus error (%)				
5	14	0	0	0	0	0
10	7	0	0	0	0	0
		C-shape : Young's modulus error (%)				
5	20.3	-14.9	-6.5	0	+10.5	17.5
10	10.1	-8.05	-3.4	0	+5.3	8.75

\*CASTEM numerical results

Calculations have been performed for different locations of extensometer rods, from -100% to 100% of operator error on the thickness face. We consider the error of operator from 0% to 100%. The magnitude of PBS along the gauge length (20 mm) is plotted versus the Young's modulus error for the two following positions : +50% and +100% (Fig. 6).

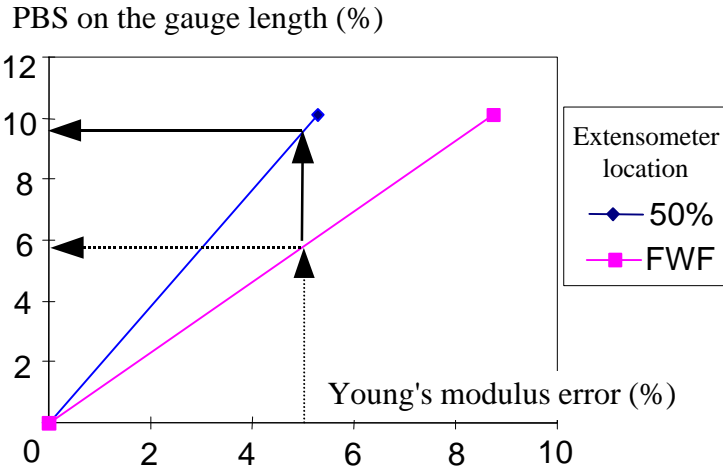


Fig 6 : PBS on the gauge length versus Young's modulus error diagram for the C-shape ( $F = 10\text{kN}$  ;  $de = 0.2\text{ mm}$ )

This diagram highlights the importance of the extensometer location when the Young's modulus is experimentally measured. The unfavourable measurement position, which is on the wide face of the specimen (position +100%), suggests a maximum PBS of about 6% if a Young's modulus error of 5% is approved (dotted arrows on Fig. 6). If the extensometer location is closer to the neutral axis (position +50%), a PBS maximum of 10% can be accepted for a Young's modulus error of 5% (solid arrows on Fig. 6).

Then, if an error of 10% is accepted for experimental measurements of the Young's modulus (which is a high level of error), a critical value of PBS of about 10% on the gauge length of 20 mm can be retained (see Fig. 6).

**Experimental procedure to measure the percent of bending**

The best procedure to measure the PBS needs to use 12 strain gauges for a rectangular specimen (see [2]). Strain gauges located at the Top and the Bottom sections are sufficient to calculate the maximum PBS along the working part. Strain gauges at the middle section give informations about the type of misalignments, S-shape or C-shape, thanks to the evaluation of the lateral displacements. But this procedure, involving the gluing of 12 strain gauges on the specimen with their longitudinal axis precisely parallel to the loading axis and several series of strain measurement, can be too heavy. In order to lighten this very precise procedure, we propose a new scheme of strain gauges implantation. This method will be called the "Alternative method" (Fig. 7).

This method needs 6 strain gauges and one rotation of 180° around the vertical axis Z. The strain values given by the strain gauges isolated on the front and on the back wide face are used two times in the calculation of the maximum PBS. Two measurements are realised : an initial measurement on the gripped specimen, and a second measurement after the rotation of the specimen. The final PBS value is the average of the two calculations. These calculations take into account an eventual imperfection of the specimen. A finite element calculation is given here after to simulate an experimental measurement of PBS on a non perfect specimen (see Table 3).

In this calculation the specimen mesh is bended with a first eccentricity defect of 0.05 mm, simulating the non perfection of the specimen. Then, this mesh is bended with an additional eccentricity defect simulating the basic eccentricity defect of the loading train (assumed for example of 0.2 mm). Hence, the first eccentricity defect applied is 0.15 mm. In this case, the eccentricity defect of the specimen is at the same side than the eccentricity defect of the loading train. The second eccentricity defect applied is -0.25 mm (simulating the rotation around the Z axis). In that case the eccentricity defect of the specimen is at the opposite side of the eccentricity defect of the loading train.

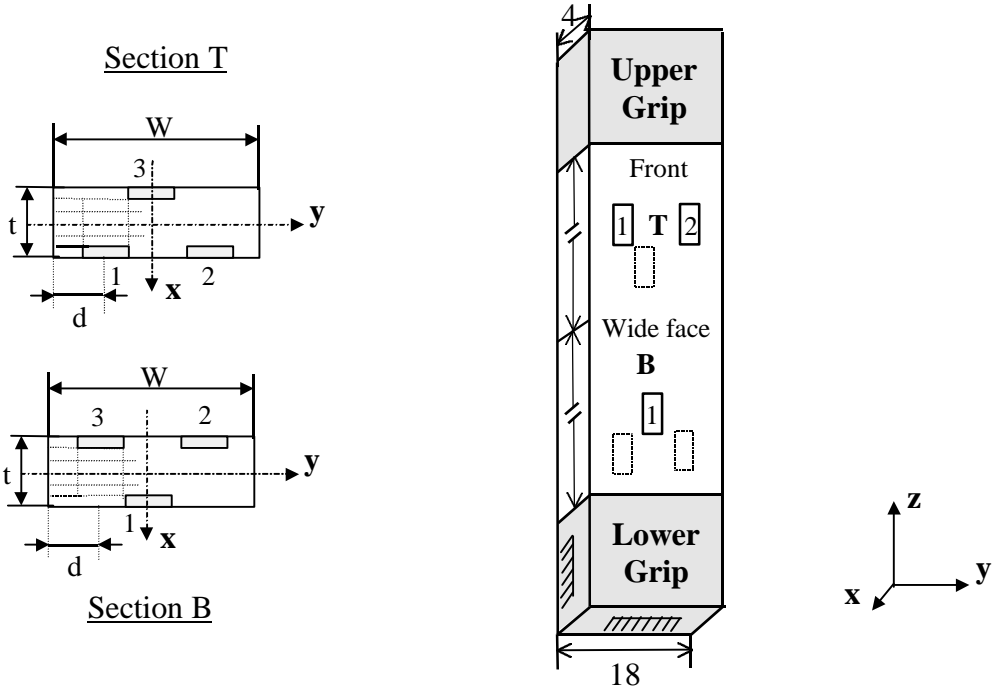


*Fig 7 : Strain gauges implantation for the "Alternative method"*

The two calculations show that the PBS value numerically evolves from a minimum to a maximum, and show that, if the specimen is non perfect, the experimental procedure of PBS evaluation needs one turn of the specimen. Then, the average value of PBS obtained is close to the value calculated for the S-shape with a perfect specimen (see Table 1 and Table 3). As a consequence, the "Alternative method" can be an acceptable procedure for the measurement of PBS on a gripped specimen.

*Table 3 : Average PBS calculated after a rotation of 180° of a non perfect specimen (S-shape, specimen defect 0.05 mm, with initial  $de = 0.2$  mm)*

$l_c = 100$ mm	Eccentricity error	
	$\underline{1} : de = 0.15$	$\underline{2} : de = -0.25$
	PBS % S-shape	
5 kN	54	92
10 kN	27	46
Average		
5 kN	73	
10 kN	36	

## CONCLUSION

This study highlights the effect of the misalignment of a gripping system on the error of measurement of the Young's modulus by mechanical tensile tests. The misalignment of grips induces a parasite bending of the specimen which have to be limited in order to have a good accuracy on the measurement of the Young's modulus of the material tested.

By numerical simulations, the relationship between the PBS and the error of measurement has been theoretically established, and a procedure of measurement of the PBS by strain gauges has been proposed. The next step of this study is to measure experimentally the PBS on specimens gripped on voluntary badly aligned testing machines, in order to confirm experimentally the theoretical relation between the PBS and the Young's modulus error. The final objective of this work is to determine the maximal admissible PBS for a given material tested under uniaxial tensile or compressive loading, and then to determine the maximum misalignment admissible for a testing machine.

## REFERENCES

1. Cambas C. "Etude des méthodes d'évaluation du non-alignement des machines à sollicitation axiale", training report C.E.A.T. (1998).
2. CEN/TC 184/SC 1 N 85 E – WI 136 “Advanced technical ceramics – Ceramic composites – Code of practice for the measurement of bending in uniaxially loaded tension-compression test specimens” (1998).